

Refinement of thermodynamic properties of ReO_2

K. Thomas Jacob^{a,*}, Saurabh Mishra^a, Yoshio Waseda^b

^aDepartment of Metallurgy and Materials Research Centre, Indian Institute of Science, Bangalore 560012, India

^bInstitute for Advanced Materials Processing, Tohoku University, Sendai 980-8577, Japan

Received 29 October 1999; accepted 7 December 1999

Abstract

The standard Gibbs energy of formation of ReO_2 in the temperature range from 900 to 1200 K has been determined with high precision using a novel apparatus incorporating a buffer electrode between reference and working electrodes. The role of the buffer electrode was to absorb the electrochemical flux of oxygen through the solid electrolyte from the electrode with higher oxygen chemical potential to the electrode with lower oxygen potential. It prevented the polarization of the measuring electrode and ensured accurate data. The $\text{Re}+\text{ReO}_2$ working electrode was placed in a closed stabilized-zirconia crucible to prevent continuous vaporization of Re_2O_7 at high temperatures. The standard Gibbs energy of the formation of ReO_2 can be represented by the equation

$$\Delta_f G^0(\text{ReO}_2)/\text{J mol}^{-1} = -451,510 + 295.011 \left(\frac{T}{\text{K}}\right) - 14.3261 \left(\frac{T}{\text{K}}\right) \ln \left(\frac{T}{\text{K}}\right) (\pm 80).$$

Accurate values of low and high temperature heat capacity of ReO_2 are available in the literature. The thermal data are coupled with the standard Gibbs energy of formation, obtained in this study, to evaluate the standard enthalpy of formation of ReO_2 at 298.15 K by the ‘third law’ method. The value of standard enthalpy of formation at 298.15 K is: $\Delta_f H_{298.15 \text{ K}}^0(\text{ReO}_2)/\text{kJ mol}^{-1} = -445.1 (\pm 0.2)$. The uncertainty estimate includes both random (2σ) and systematic errors. © 2000 Elsevier Science B.V. All rights reserved.

Keywords: Gibbs energy of formation; Enthalpy; Entropy; Advanced solid-state cell; Micropolarization

1. Introduction

ReO_2 is used in a number of device applications. It is used in the fabrication of the bottom electrode in integrated ferroelectric capacitors [1]. The electrode consisting of thin films of a nitride, Pt and ReO_2 is resistant to peeling [1]. A layer containing Re and

ReO_2 can be used to protect substrate regions, Si-containing layers, dielectric layers, electrodes, barrier layers, contact and via plugs, inter-connects and ferroelectric capacitors [2]. The layer is capable of being oxidized or reduced preferentially to an adjacent region of the device. Thermodynamic data on ReO_2 are useful for the evaluation of interface stability during high-temperature processing of device structures.

The rhenium–oxygen binary system has three solid oxides, ReO_2 , ReO_3 and Re_2O_7 [3]. Re_2O_7 melts at 573 K and boils at 633 K [4]. ReO_3 crystallizes in the

* Corresponding author. Fax: +91-80-334-9472, +91-80-334-1683.

E-mail addresses: katob@metallrg.iisc.ernet.in (K.T. Jacob), katob@mrc.iisc.ernet.in (K.T. Jacob)

Table 1
Summary of measurements of $\Delta_f G^0(T)$ (ReO₂) and derived $\Delta_f H^0(298.15\text{ K})$

Author	$\Delta_f G^0(T)$ (ReO ₂)/J mol ⁻¹	T/K	Method	$\Delta_f H^0$ (298.15 K)/ kJ mol ⁻¹	'Third law' drift/kJ mol ⁻¹
Franco and Kleykamp [7]	$-438,650+180.749(T/K)$	850–1130	emf (Fe+FeO ref.)	-447.5	±0.1
Pownceby and O'Neill [8]	$-451,020+297.595(T/K)$ $-14.6585(T/K) \ln(T/K)$	850–1250	emf (Ni+NiO and Cu+Cu ₂ O ref.)	-444.35	±0.01
This study	$-451,511+295.001(T/K)$ $-14.3261(T/K) \ln(T/K)$	900–1200	emf (O ₂ ref., buffer electrode, encapsulation)	-445.139	±0.005

cubic system with lattice parameter $a=0.3751\text{ nm}$ [5]. At higher temperatures, ReO₂ is the only stable solid oxide. There are two forms of ReO₂: a monoclinic variety with MoO₂-type structure (space group P2₁/c) stable at lower temperatures, and an orthorhombic form (space group *Pbcn*) with four formula units per cell [6] stable at high temperatures. The lattice parameters of the orthorhombic form are: $a=0.48094\text{ nm}$, $b=0.56433\text{ nm}$, $c=0.46007\text{ nm}$ [5].

There are two earlier investigations of the Gibbs energy of the formation of ReO₂ using solid-state electrochemical techniques and secondary reference standards [7,8]. The results are summarized in Table 1. The results from the two studies differ by ca. 3 kJ mol⁻¹. The vapor pressure of Re₂O₇ over the mixture Re+ReO₂ is significant at high temperature. Battles et al. [9] have investigated the vapor pressure of Re₂O₇ over the two-phase mixture Re+ReO₂ in the temperature range from 960 to 1080 K by combined mass loss and mass spectrometric Knudsen effusion studies. Franco and Kleykamp [7] used a glass-sealed (Y₂O₃)ZrO₂ electrolyte crucible for their measurements to prevent vaporization of Re₂O₇ from their working electrode. Franco and Kleykamp [7] have reviewed the older literature on the Re–O system. In this article, only those publications that directly contribute to the evaluation of accurate data for ReO₂ are discussed. A solid-state galvanic cell incorporating advanced features such as the buffer electrode and encapsulated working electrode is used in this study to obtain very accurate data on the high-temperature Gibbs energy of the formation of ReO₂. Pure oxygen gas at a pressure of 0.1 MPa is used as the reference electrode.

Both low- and high-temperature heat capacities of ReO₂ (8–1400 K) have been measured accurately by

Stuve and Ferrante [10]. This gives an accurate value of 47.83 J K⁻¹ mol⁻¹ for the standard entropy of ReO₂ at 298.15 K. This information is coupled with the high-temperature Gibbs energy of formation measured in this study, and auxiliary information on other phases available in the literature, to derive the standard enthalpy of formation using the 'third-law' method.

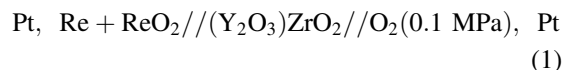
2. Experimental aspects

2.1. Materials

Fine powders of Re and ReO₂ used in this study were of 99.99% purity. They were characterized by XRD.

2.2. Measurement of the Gibbs energy of formation

The reversible emf of the following solid-state cell was measured as a function of temperature:



The cell is written such that the right hand electrode is positive. Due to the difference in the chemical potential of oxygen between the reference on the right side and working electrode on the left side of the cell, there is always a small flux of oxygen through the zirconia electrolyte separating them, even in the absence of physical porosity [11]. Even in the predominantly ionic conduction domain ($t_{\text{ion}} > 0.99$) of the solid electrolyte, there are small, but infinite, values for electron and hole conductivity. The electrochemical permeability is caused by the coupled transport of oxygen ions and holes (or electrons) in the solid electrolyte

under the oxygen potential gradient. Only opposing it with an external dc voltage exactly equivalent to the oxygen chemical potential difference can stop this small, but significant, flow of oxygen [12]. The coupled flow of charged species is equivalent to a high-resistance internal short circuit.

The electrochemical flux of oxygen would cause micropolarization of multiphase solid electrodes. The chemical potential of oxygen in the microsystem near the solid electrode/electrolyte interface would be altered because of the semi-permeability of the electrolyte to oxygen. A buffer electrode, introduced between reference and working electrodes, was designed to act as a sink for the oxygen flux and prevent the flux from reaching the working electrode. The buffer electrode was maintained at an oxygen chemical potential close to that of the working electrode. Since there was no significant difference between the chemical potentials of the buffer and working electrodes, the driving force for the transport of oxygen through the zirconia tube separating these electrodes did not exist. The working electrode therefore remained unpolarized. Pure oxygen gas, at a pressure of 0.1 MPa and flowing over a platinized surface of zirconia, constituted the primary reference standard for oxygen potential and formed an unpolarizable electrode. Thus, the three-electrode design of the cell prevented error in emf caused by the polarization of the working electrode. Measuring the emf between the buffer and the working electrodes assessed the magnitude of the polarization effect. Transport of oxygen between the electrodes through the gas phase was prevented by the physical isolation of the gas phase over the three electrodes.

The cell design used for high-temperature emf measurements consisted of three distinct compartments, separated by two impervious yttria-stabilized zirconia tubes or crucibles. The cell can be represented schematically as follows:

Working electrode O ₂ (P' _{O₂}), Pt	(Y ₂ O ₃)ZrO ₂ No flux	Buffer electrode O ₂ (P'' _{O₂}), Pt P'' _{O₂} ≈ P' _{O₂}	(Y ₂ O ₃)ZrO ₂ ← O ²⁻	Reference electrode O ₂ (0.1 MPa), Pt
------------------------------------------------------------------------	-------------------------------------------------------------	--------------------------------------------------------------------------------------------------------------------------------------	-----------------------------------------------------------------------	-----------------------------------------------------

The apparatus used initially for the measurement of the oxygen potential corresponding to Re+ReO₂ equilibrium was similar to that described earlier [13]. When measurements on the Re+ReO₂ electrode were

conducted, some condensation of Re₂O₇ was observed on the cooler parts of the apparatus, suggesting the presence of a volatile species over the working and buffer electrodes. The vapor pressure of the Re₂O₇ gas species in equilibrium with Re and ReO₂ can be computed from the thermodynamic data given in the compilation of Knacke et al. [14]:

$$\ln\left(\frac{P_{\text{Re}_2\text{O}_7}}{P^0}\right) = \frac{-51,770}{(T/\text{K})} + 37.906. \quad (2)$$

The vapor pressure of Re₂O₇ in equilibrium with Re+ReO₂ becomes significant at high temperature. Hence, the apparatus for the measurements on Re+ReO₂ was redesigned as shown in Fig. 1. The Re+ReO₂ working electrode was contained in the closed crucible of the yttria-stabilized zirconia. A Pt O-ring provided a gas-tight seal between the crucible and an alumina lid. The Re lead was introduced through a small hole in the lid. The gap around the lead was closed with a glass seal.

The Pt group metals readily form alloys. When Pt is placed in contact with the Re+ReO₂ electrode, alloy formation can increase the oxygen potential in the immediate vicinity of the alloy. Hence, a short length of Re wire was used as the contact lead to the Re+ReO₂ electrode. The Re/Pt junction was made at a small distance from the working electrode. Since the joints between Re and Pt wires were located in the even temperature zone, there was no significant thermoelectric contribution to the emf from this source.

The buffer electrode of Re+ReO₂ in the molar ratio 1:1 was contained in the larger zirconia crucible. The electrode was covered with a layer of zirconia powder to minimize the evaporation of Re₂O₇ from the electrode. Electrical contact to the Re+ReO₂ buffer electrode was made by a short wire of Re metal, spot-welded to a Pt lead.

The zirconia crucible containing the buffer electrode rested on another inverted zirconia tube. The

mating surfaces of the crucible and tube were polished with diamond paste to minimize contact resistance. The inside surface of the inverted zirconia tube was platinized. Platinum gauze was pressed against the

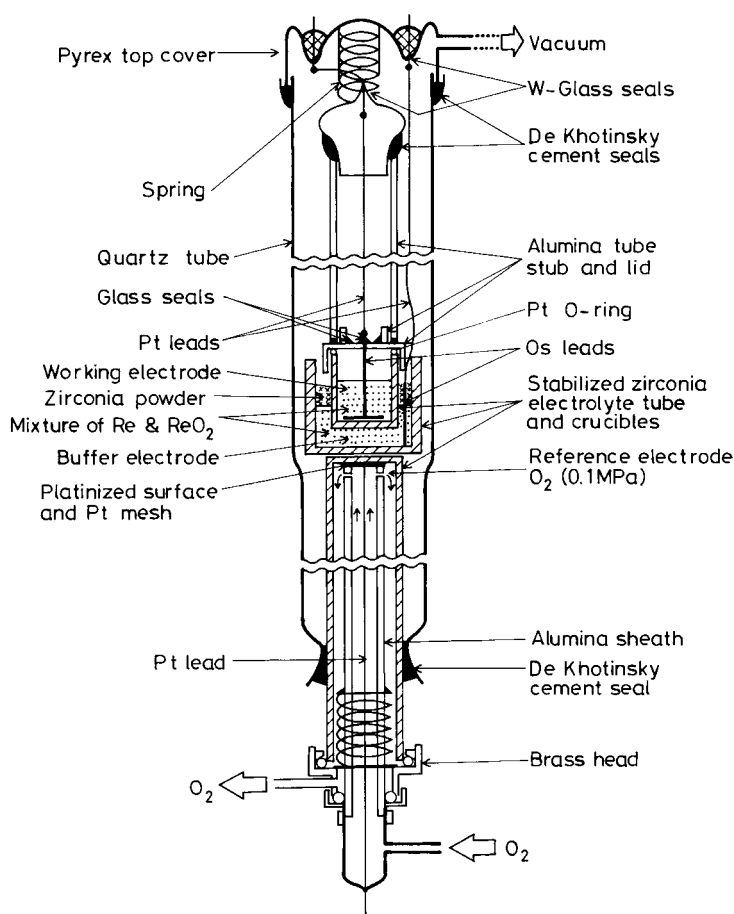


Fig. 1. A schematic diagram of the new apparatus for high-temperature emf measurements, with the working electrode in a closed crucible and a buffer electrode interspersed between reference and working electrodes.

closed end of the inverted tube, using an alumina sheath. A Pt lead, spot-welded to the gauze, passed through the alumina sheath. The open end of the inverted zirconia tube was fitted with a brass head. Pure oxygen gas at a pressure of 0.1 MPa was flowed through the inverted zirconia tube at a rate of 3 ml/s. A cascade of bubblers placed at the gas exit controlled the pressure inside the tube. The oxygen electrode served as the reference. In all other respects, the assembly and use of the apparatus were identical to that described in detail in an earlier article [13].

The entire assembly shown in Fig. 1 was placed inside a vertical resistance furnace, with the electrodes located in the even temperature zone (± 1 K). The upper and lower parts of the assembly, where cement

seals were located, remained at room temperature during the measurements. A Faraday cage made from thick stainless steel foil was placed between the furnace and the cell assembly. The foil was grounded to minimize induced emf on cell leads. The temperature of the furnace was controlled to ± 1 K. The temperature was measured by a Pt/Pt-13% Rh thermocouple, checked against the melting point of gold. All temperatures are based on ITS-90. The cell potentials were measured with a high-impedance digital voltmeter with a sensitivity of ± 0.01 mV. The potential readings were corrected for small thermal emfs, measured separately using a symmetric cell with identical electrodes. At the end of each experiment, the electrodes were cooled to room temperature and examined

by optical and scanning electron microscopy and XRD. Although small changes in the relative concentration of the constituents were observed, the number and nature of the phases remained unaltered. The change in relative concentration was consistent with the expected decomposition of ReO_2 at high temperature to generate the equilibrium oxygen pressure in sections of the apparatus.

3. Results and discussion

3.1. Gibbs energy of formation of ReO_2

The reversible emf of the cell is plotted as a function of temperature in Fig. 2. The emf was measured in the temperature range of 900–1200 K using a novel apparatus incorporating a buffer electrode. It was difficult to extend the measurements beyond 1200 K. The reversibility of the emf was established by microcoulometric titration in both directions. A small current (ca. 50 μA) was passed through the cell, using an external potential source for ca. 200 s, and the open-circuit emf was subsequently monitored as a function

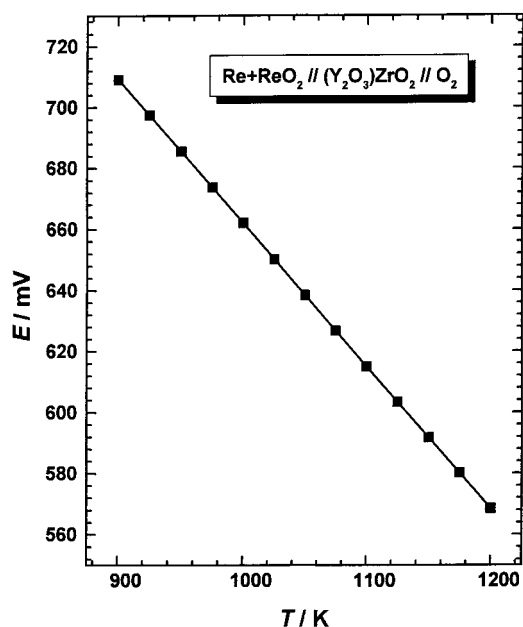


Fig. 2. The reversible emf of the solid-state cell as a function of temperature.

of time. The emf was found to return to the steady value before each perturbation. During each titration, the chemical potential of oxygen at each electrode was displaced from equilibrium by an essentially infinitesimal amount. Since the electrodes returned to the same potential after such displacements in opposite directions, the equilibrium was experimentally verified. The emf was not affected by the flow rate of oxygen through the reference electrode in the range of 2–5 ml s^{-1} . The emfs were also found to be reproducible on temperature cycling.

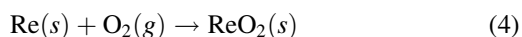
With the three-electrode design of the cell, the emfs were steady (± 0.15 mV) for periods in excess of 40 ks. The emf of the buffer electrode measured against the reference was almost identical to that of the working electrode at the beginning of the experiment. The emf between the buffer and reference electrodes was ca. 2 mV lower than that between the working and reference electrodes at temperatures below 1050 K, and ca. 2.5 mV higher at 1200 K. The lower emf is indicative of polarization of the buffer electrode. When zirconia powder was not used to cover the $\text{Re}+\text{ReO}_2$ mixture at the buffer electrode, the difference at high temperature increased to ca. 4 mV. This suggests that the lower oxygen chemical potential at the buffer electrode at high temperature may be related to the vaporization of Re_2O_7 .

The reversible emf plotted in Fig. 2 varies non-linearly with temperature. The emf can be represented by the equation (temperature range: 900 to 1200 K):

$$\frac{E_1}{\text{mV}} = 1169.9 - 0.76437 \left(\frac{T}{\text{K}} \right) + 0.03712 \left(\frac{T}{\text{K}} \right) \times \ln \left(\frac{T}{\text{K}} \right) (\pm 0.2)$$

where E_1 is the emf of the solid-state cell. The coefficients were obtained by non-linear regression analysis using a pre-selected expression for emf. The expression is based on a constant value of ΔC_p^0 for the cell reaction. The uncertainty estimate is based on both systematic and random (2σ) errors, where σ is the standard error estimate. Since pure Re and ReO_2 are present at unit activity at the working electrode, the standard Gibbs energy of the formation of ReO_2 is related to the oxygen chemical potential at the electrode. As pure oxygen at 0.1 MPa is used as the

reference electrode, the emf is directly related to the standard Gibbs energy of formation, $\Delta_f G^0$ (ReO_2), by the Nernst equation, $\Delta_f G^0 = -4FE_1$, where F is the Faraday constant. For the reaction,



$$\begin{aligned} \Delta_f G^0(\text{ReO}_2)/\text{J mol}^{-1} \\ = -451,510 + 295.011 \left(\frac{T}{\text{K}}\right) \\ - 14.3261 \left(\frac{T}{\text{K}}\right) \ln\left(\frac{T}{\text{K}}\right) (\pm 80) \end{aligned} \quad (5)$$

The standard Gibbs energy of the formation of ReO_2 obtained in this study is compared in Fig. 3 with values from earlier measurements [7,8] and compilations [14–16]. The differences between the values reported in the literature and those obtained in this study are plotted as a function of temperature. The results of Franco and Kleykamp [7] are more negative by ca. 2.2 kJ mol^{-1} than the results obtained in this study. As Franco and Kleykamp used $\text{Fe} + \text{FeO}$ as the reference electrode, their emfs were slightly

lower than would be expected. This is probably caused by the polarization of their electrodes. Values given in the compilations of Barin [15] and Pankratz [16] are influenced by the results of Franco and Kleykamp. The values given in the compilation of Knacke et al. [14] are higher by ca. 3.8 kJ mol^{-1} . The recent study of Pownceby and O'Neill [8], using $\text{Ni} + \text{NiO}$ and $\text{Cu} + \text{Cu}_2\text{O}$ as the reference electrodes, is in good agreement with the data obtained in this study. Their results are more positive by ca. 0.8 kJ mol^{-1} over the entire temperature range. This small difference may be attributed to uncertainties associated with their reference standards. The results obtained by Pownceby and O'Neill [8] using the two reference electrodes ($\text{Ni} + \text{NiO}$ and $\text{Cu} + \text{Cu}_2\text{O}$) show some difference.

The standard enthalpy of formation of ReO_2 at 298.15 K can be evaluated from the results obtained in this study by the ‘third-law’ method, based on the equation:

$$\begin{aligned} \Delta_f H^0(298.15 \text{ K}) \\ = \Delta_f G^0(T) - \int_{298.15}^T \Delta C_p^0 dT \\ + T \left[\Delta_f S^0(298.15 \text{ K}) + \int_{298.15}^T \frac{\Delta C_p^0}{T} dT \right] \end{aligned} \quad (6)$$

where the changes in the thermodynamic parameters are defined for the formation of ReO_2 from elements according to reaction (4). The ‘third-law’ analysis is based on the knowledge of the absolute entropy of the reactants and products at 298.15 K. For solid materials, this requires measurement of low-temperature heat capacity. Furthermore, high-temperature heat capacity of reactants and products should be available. Then, the ‘third-law’ analysis allows us to calculate the standard enthalpy change for the reaction at 298.15 K from each value of the Gibbs energy of formation at high temperature. When all the data are correct, the derived enthalpy change is independent of the temperature of measurement of the Gibbs energy of formation. A drift with temperature of the derived enthalpy change at 298.15 K indicates error in at least one set of input data.

An analysis of the Gibbs energy of formation of ReO_2 obtained in this study, along the lines suggested above, yields the average value for standard enthalpy

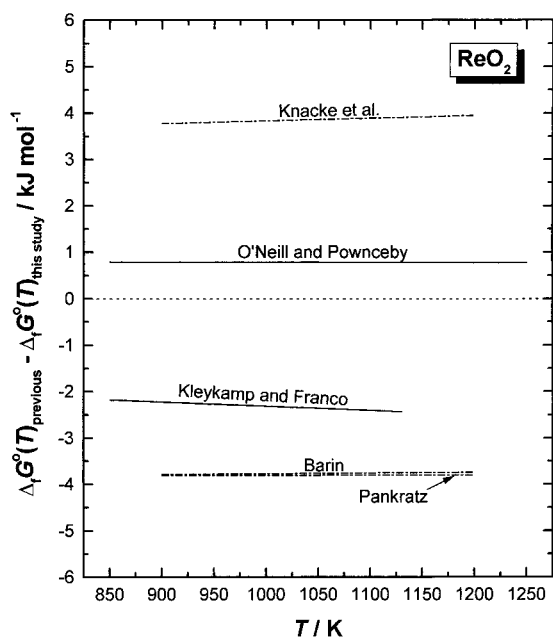


Fig. 3. A comparison of the Gibbs energy of the formation of ReO_2 . The difference between the value reported by other investigators and that obtained in this study is plotted as a function of temperature.

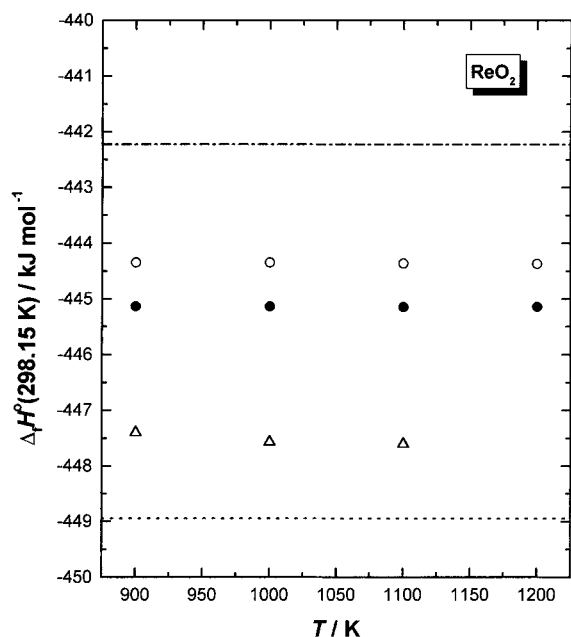


Fig. 4. Results of the 'third-law' analysis of high-temperature data on standard Gibbs energy of the formation of ReO_2 . (Δ) Franco and Kleykamp [7]; (\circ) Pownceby and O'Neill [8]; (\bullet) this Study. Data in the compilations are shown by lines; (\cdots) Barin [14] and Pankratz [15], ($- - -$) Knacke et al. [13].

of formation at 298.15 K, $\Delta_f H_{298.15 \text{ K}}^0(\text{ReO}_2)/\text{kJ mol}^{-1} = -445.14$, with a drift of only $\pm 0.005 \text{ kJ mol}^{-1}$, as shown in Table 1. Both low- and high-temperature heat capacities of ReO_2 from 8 to 1400 K have been measured accurately by Stuve and Ferrante [10]. This gives an accurate value of $47.83 \text{ J K}^{-1} \text{ mol}^{-1}$ for the standard entropy of ReO_2 at 298.15 K. Auxiliary data for Re and O_2 from Pankratz [16] were used in the 'third-law' analysis.

A re-analysis of the Gibbs energies of formation reported in the literature [7,8], by the 'third law' method using the same thermal functions, gives values displayed in Fig. 4. The results of this study are in fair agreement with values obtained from Pownceby and O'Neill [8]. The present results, based on a more accurate measurement of the Gibbs energy of formation using an advanced version of the solid-state cell, refine the values suggested by Pownceby and O'Neill [8]. The value of $\Delta_f H_{298.15 \text{ K}}^0(\text{ReO}_2) = -445.14 \text{ kJ mol}^{-1}$ obtained by 'third-law' analysis is significantly better than the value of $-448.943 \text{ kJ mol}^{-1}$ suggested

in the compilations of Barin [15] and Pankratz [16], and $-442.223 \text{ kJ mol}^{-1}$ in Knacke et al. [14], based on old information.

4. Conclusions

Presented in this article is a precise measurement of the thermodynamic properties of ReO_2 using a solid-state cell with a buffer electrode, which prevents the polarization of the electrodes caused by the electrochemical transport of oxygen through the electrolyte. The buffer electrode absorbs the oxygen flux from the oxygen reference electrode to the measuring electrode, and thus prevents it from disturbing the working electrode. The working electrode was contained in a closed cell to prevent the escape of Re_2O_7 gas. The heat capacity of ReO_2 from 8 to 1400 K have been measured accurately by Stuve and Ferrante [10]. This gives an accurate value of $47.83 \text{ J K}^{-1} \text{ mol}^{-1}$ for the standard entropy of ReO_2 at 298.15 K. This information was coupled with the precise measurement of the Gibbs energy of the formation of ReO_2 at high temperature, and auxiliary data available in the literature for Re and O_2 , to get a refined value for the enthalpy of formation at 298.15 K: $\Delta_f H_{298.15 \text{ K}}^0(\text{ReO}_2)/\text{kJ mol}^{-1} = -445.1 (\pm 0.2)$. The results of this study suggest a minor revision of values given in current thermodynamic compilations.

References

- [1] M. Osata, Y. Ogimoto, H. Matsunaga, *Jpn. Kokai Tokyo Koho JP.*, 10, 56 140 (1998) 7 pp.
- [2] D.P. Maniar, R. Moazzami, J.C. Mogab, *Eur. Pat. Appl. EP* 629,002 (1994) 15 pp.
- [3] R. Colton, *The Chemistry of Rhenium and Technetium*, Interscience Publishers, New York, 1965, pp. 33–52.
- [4] W.T. Smith Jr., L.E. Line Jr., W.A. Bell, *J. Am. Chem. Soc.* 74 (1952) 4964.
- [5] A. Magneli, *Acta Chem. Scand.* 11 (1957) 28–33.
- [6] A. Magneli, *Acta Cryst.* 9 (1956) 1038–1039.
- [7] J.I. Franco, H. Kleykamp, *Ber. Bunsenges. Phys. Chem.* 75 (1971) 934–938.
- [8] M.I. Pownceby, H.S.C. O'Neill, *Contrib. Mineral. Petrol.* 118 (1994) 130–137.
- [9] J.E. Battles, G.E. Gundersen, R.K. Edwards, *J. Phys. Chem.* 72 (1968) 3963.
- [10] J.M. Stuve, M.J. Ferrante, *U.S. Bureau of Mines, RI* 8199 (1976) 15 pp.

- [11] J. Fouletier, P. Fabry, M. Kleitz, *J. Electrochem. Soc.* 123 (1976) 204.
- [12] K.T. Jacob, J.H.E. Jeffes, *Trans. Inst. Min. Metall. (London), Sec. C* 80 (1971) C181.
- [13] K.T. Jacob, T.H. Okabe, T. Uda, Y. Waseda, *J. Electrochem. Soc.* 146 (1999) 1854.
- [14] O. Knacke, O. Kubaschewski, K. Hesselmann, *Thermochemical Properties of Inorganic Substances I & II*, Springer-Verlag, Berlin, Germany, 2nd Edition, 1991, pp. 1672, 1676–1680.
- [15] I. Barin, *Thermochemical Data of Pure Substances, Parts I & II*, VCH, Weinheim, Germany, 1989.
- [16] L.B. Pankratz, *Thermodynamic Properties of Elements and Oxides*, Bull. 672, U.S. Department of the Interior, Bureau of Mines, Washington DC, 20402, 1982.